Astron. Astrophys. 332, 767–774 (1998)

ASTRONOMY
AND
ASTROPHYSICS

Two-dimensional spectral observations of sunspots in chromospheric lines

I. Asymmetries of Ca II lines

M.D. Ding[1,2] **and H. Schleicher**[2]

[1] Department of Astronomy, Nanjing University, Nanjing 210093, P.R. China
[2] Kiepenheuer-Institut für Sonnenphysik, Schöneckstrasse 6, D-79104 Freiburg, Germany

Received 2 January 1997 / Accepted 19 December 1997

Abstract. We present two-dimensional spectral observations of two closely located small sunspots in chromospheric lines. Line asymmetries and shifts are derived for the Ca II K line in particular. It is found that the majority of Ca II K profiles show a blue asymmetry. Red asymmetry may also appear, but only in some tiny regions. Some ephemeral blue asymmetry patches are found in the umbrae, which seem to be related to umbral flashes. On the limb side of the penumbra, the Ca II K profiles show a distinguishably blue asymmetry of K_1. In contrast, the profiles on the center side are more likely to possess a blue asymmetry of K_2, together with a slight red shift of K_3. We discuss possible causes for such a peculiar spatial distribution of line asymmetries. Further line profile computations are needed to get a consistent and satisfactory explanation.

Key words: line: profiles – sunspots

1. Introduction

The Ca II lines have been extensively studied in the last three decades to understand the physical conditions in the solar chromosphere. Due to their various core emission features, the Ca II resonance lines (H and K) are now widely used as probes of chromospheric dynamics as well as lines for model computations. Many quiet Sun spectra with high spatial resolution revealed that the core emission of these lines shows a great variability, i.e., single-peaked or double-peaked (self-reversed), blue-asymmetric or red-asymmetric, with or without a line center shift (e.g., Pasachoff 1970; Liu & Smith 1972; Grossmann-Doerth et al. 1974). Attempts have been made to explain the observed Ca II H (K) emission features. Many authors interpreted the line asymmetries and shifts as a consequence of upward propagation of acoustic waves which are initially excited in or below the photosphere (e.g., Heasley 1975; Cram 1976; Durrant et al. 1976; Gouttebroze & Leibacher 1980).

In particular, spectral observations in sunspots have received much attention. Detailed analyses of lines formed in the chromosphere of sunspot umbrae were carried out by Mattig & Kneer (1978) and Kneer et al. (1981a). Observations in multiple lines were also made by Kneer et al. (1981b) and Vial & Bellout (1987). Lites (1986, 1988) observed time sequences of line profiles to investigate the oscillation behavior in sunspot umbrae and penumbrae. The most conspicuous phenomenon detected in umbrae is the umbral flash, where the lines show periodic temporal brightenings and great asymmetries (Kneer et al. 1981a). It is well known that, on the average, the umbral Ca II H (K) line has a single emission peak while the penumbral line exhibits double peaks. However, there is evidence that the umbral fine structures exhibit as much line shape variation as the fine structures of the quiet Sun, even though there is a big difference in their absolute line intensities and in their distribution ratios of each kind of variation.

As for the line asymmetries, we could find some similarities between the sunspot and quiet Sun lines, but this does not necessarily mean that their causes are the same. The sunspot represents a highly magnetized area showing dynamics (oscillations, waves, and systematic flows) quite different from the undisturbed region. In particular, there exists the well known Evershed flow in the penumbra. In addition, it has been discovered that during the sunspot decay, magnetic elements appear to move outward from the spot boundary, which are known as "moving magnetic features" (see e.g., Harvey & Harvey 1973; Nye et al. 1984).

The purpose of this project was to obtain 2D spectral observations of a sunspot in multiple chromospheric lines with high spatial and spectral resolutions. Such observations enable us to study in detail the spatial distribution of different line features in the sunspot area and to gain insight into the atmospheric condition and dynamic behavior of the chromosphere above the sunspot. In the following sections, we describe the observations

Send offprint requests to: H. Schleicher

and data reduction in Sect. 2. The results and discussions are presented in Sect. 3. A brief conclusion is drawn in Sect. 4.

2. Observations and data reduction

2.1. Observations

The observations were carried out on June 8, 1996, using the German Vacuum Tower Telescope (VTT) at Tenerifa, Spain. The detailed optics for this telescope can be found in Soltau (1983). The object for spectral observations was a pair of small sunspots closely located. The distance between the two umbrae was $\sim 10''$ and the center position of them was N05 W25. These twin spots shared a same magnetic polarity. The seeing during observations was quite good and estimated to be $\sim 1''$.

The 2D spectral observations were achieved using a fixed slit spectrograph and moving the target of interest stepwise across the slit. The 2D spectra obtained in this way are certainly not simultaneous. In order to minimize the non-simultaneity and not to lose the spatial resolution in the mean time, we set the stepping size to be $1''$, a value nearly equal to the seeing. 50 steps were used for one complete scan, but only half of them covered the sunspots. The time interval between successive steps was 15 s, which was required for camera exposing, data recording, and image moving.

The program was originally designed to observe three lines (Hα, Ca II K and 8498) simultaneously. Due to the large wavelength difference, the slit direction was set at 65° west to north, an optimum position to avoid image shifts perpendicular to the slit direction due to differential refraction. Three 1024×1024 CCD cameras were operated simultaneously for the three lines. After 2×2 binning, one frame of slit spectra contains a 512×512 data array, whose pixel size is $0\farcs187$ along the slit, 2.4 mÅ for Ca II K and 5 mÅ for Ca II 8498 along the dispersion. To get enough counts and avoid the CCD saturation, the exposure time was selected to be 4 s for Ca II K but 0.5 s for the other two lines. Unfortunately, during the observations, there appeared some technical problems which made the Hα spectra unreliable (one wing was seriously darker than the other wing). We therefore do not analyze this line in the present work.

The observations began at $\sim$ 08 : 00 UT and ended at $\sim$ 12 : 30 UT. During this period, we performed in total 12 scans. Finally, the dark current and the flat field were measured. The latter was done at disk center by defocusing and circularly moving the solar image to smear out the inhomogeneities.

2.2. Data reduction

For each CCD camera, we obtained the dark current matrix by averaging the measurements of over 10 times. The gain matrix was calculated by normalizing the flat field spectra (rows in the data array) to a mean spectrum. With the available dark current and gain matrices, all the recorded count rates were then converted into relative intensities. Before doing that, a possible tilt of the slit relative to the CCD columns must be removed by rotating the observed data array for an appropriate angle. We did not perform any stray light correction. This should have no great influence for the following discussions as our main interest is the line asymmetry. In Sect. 3.3, we will further justify this assumption.

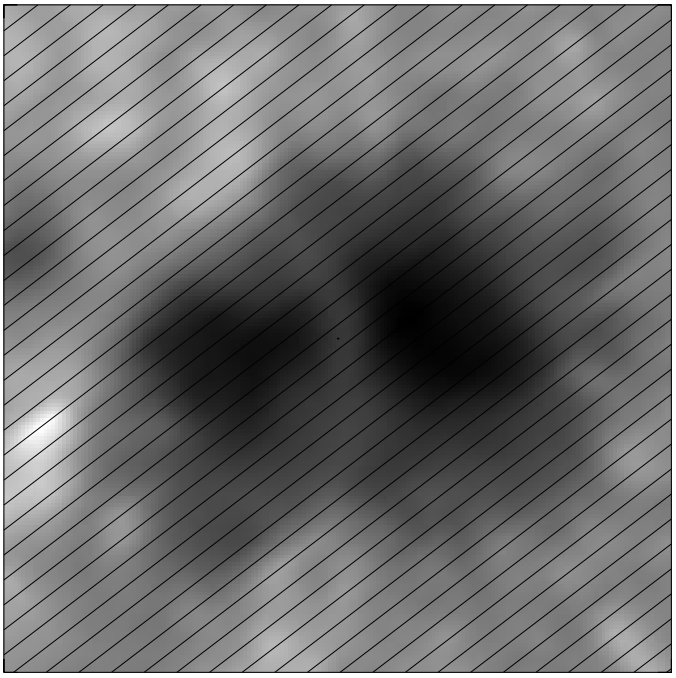

Fig. 1. An example of the sunspot image at Ca II K wing ($\Delta\lambda$ = 0.52 Å) reproduced from the 2D scanning spectra. The middle time of the scan is 10:01 UT. Overlapped slanted lines are slit positions. The field of view is $33\farcs6 \times 33\farcs6$. North is up. West is to the right

To compare images at different lines and at different times, some coalignment has been done to compensate for the refraction effect along the slit direction and image drifts during observations. We did this by shifting an image relative to a target image and finding out the position with a maximum cross-correlation coefficient. Of course, only line wing images can be used in this procedure. As an example, Fig. 1 displays the image of sunspots at Ca II K wing ($\Delta\lambda$ = 0.52 Å), which was scanned at around 10:01 UT. The image has been rotated to give the usual orientation. The overlapped thin lines mark the slit positions in this scan.

3. Results and discussions

The present work is concentrated on studying the asymmetry property of the Ca II lines. As usual, denote for the Ca II K line by I and λ its relative intensity and wavelength, and by subscripts K_{1v}, K_{1r}, K_{2v}, K_{2r}, and K_3 the blue wing minimum, red wing minimum, blue wing maximum, red wing maximum, and the line center, respectively. K_3 represents the central absorption for double-peaked (DP) line cores but the emission peak for single-

peaked (SP) line cores. The following asymmetry parameters are computed:

$$A_0 = 2\left(\int_{\lambda_{\rm K1v}}^{\lambda_0} I_\lambda {\rm d}\lambda - \int_{\lambda_0}^{\lambda_{\rm K1r}} I_\lambda {\rm d}\lambda\right) \Big/ \int_{\lambda_{\rm K1v}}^{\lambda_{\rm K1r}} I_\lambda {\rm d}\lambda\,, \quad (1)$$

$$A_1 = 2(I_{\rm K1v} - I_{\rm K1r})/(I_{\rm K1v} + I_{\rm K1r})\,, \quad (2)$$

$$A_2 = 2(I_{\rm K2v} - I_{\rm K2r})/(I_{\rm K2v} + I_{\rm K2r})\,, \quad (3)$$

and

$$A_3 = -\Delta\lambda = -(\lambda_{\rm K3} - \lambda_0)\,, \quad (4)$$

where λ_0 is the line center wavelength of a reference profile (we use the flat field profile here). A_0 is a measure of the difference in line fluxes integrated in the blue part and in the red part of the emission core. It contains the effects of A_1 and A_2, and is possibly influenced by variations of $\lambda_{\rm K1v}$ and $\lambda_{\rm K1r}$. Note that A_2 is only computed for DP lines. As the Ca II 8498 line shows pure absorption in most cases, we only consider the Doppler shift of the line bisector.

3.1. A statistics of asymmetric line profiles

To get a general view of the asymmetry of sunspot Ca II K lines, we plot in Fig. 2 the distribution of lines according to A_2 for DP profiles and to A_3 for SP profiles. We do not distinguish the umbral and penumbral profiles in this statistics, but it is conceivable that penumbral profiles fall mostly into the first category while umbral profiles fall mainly into the second category. Four scans with relatively better seeing, out of 12 in total, are plotted in the figure.

It is clear that in sunspots, the vast majority of Ca II K profiles show a blue asymmetry. That is to say, for DP profiles, the blue peak is usually brighter than the red peak; while for SP profiles, the emission peak tends to be shifted blueward. One can find, however, a small number of profiles showing the opposite behavior.

In addition, it can be seen that the distribution shape of SP profiles changes somewhat with time. For example, the 09:14 and 11:11 UT cases exhibit more profiles with large blue shifts ($A_3 > 0.05$ Å), while the 12:01 UT case has less such profiles but more profiles with red shifts ($A_3 < 0$). Although it is difficult to study in detail such a temporal variation due to the lack of time resolution, we regard it as a phenomenon related to umbral flashes (Kneer et al. 1981a), based on the spatial distribution of A_0 displayed in Fig. 4. On the contrary, no significant change is detected for the distribution of DP profiles.

To get a deeper impression of Ca II K line profiles, we plot in Fig. 3 four profiles with different asymmetries selected from one scan (10:01 UT). They only represent typical cases of asymmetries of K_2 or shifts of K_3 but not asymmetries of K_1 which will be discussed below.

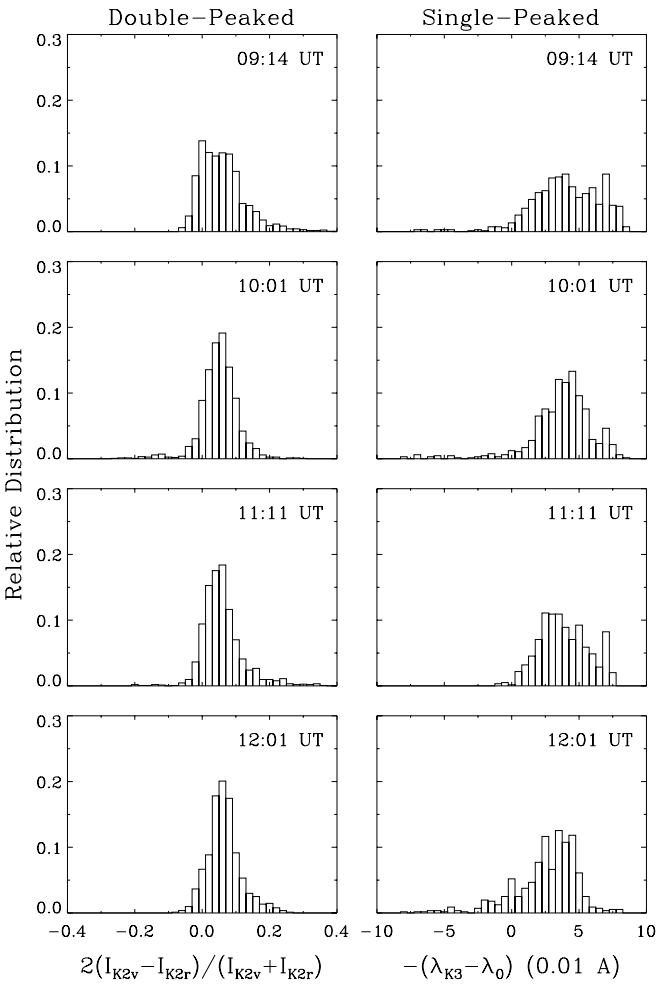

Fig. 2. Distributions of sunspot Ca II K lines according to the asymmetry parameters A_2 for DP profiles (left column) and A_3 for SP profiles (right column). Four scans out of 12 in total are plotted

3.2. The spatial distribution of asymmetry parameters

Fig. 4 displays the spatial distribution of A_0 in the whole observed region for the same four scans as in Fig. 2. For clarity, blue asymmetry (positive A_0) and red asymmetry (negative A_0) are shown in the left and right columns independently. Both of them are in gray scale, with darkness 1 corresponding to $A_0 = \pm 0.30$ and darkness 0 to $A_0 = \pm 0.05$. The solid curves delineate the inner and outer penumbral boundaries, which are drawn as intensity contours at Ca II K wing ($\Delta\lambda = 0.52$ Å), with the two contour levels being mean intensities averaged over the umbra and penumbra, and over the penumbra and quiet region, respectively. We have no spectral data at the visible continuum. Compared with the video record, such contours match well the real boundaries.

First of all, we notice that the blue asymmetries preferentially appear on the limb side of the spots. The asymmetry strip follows approximately the outer penumbral boundary. It occupies a large fraction of the limb side penumbra and also stretches into the quiet region. During the observation time of nearly 3

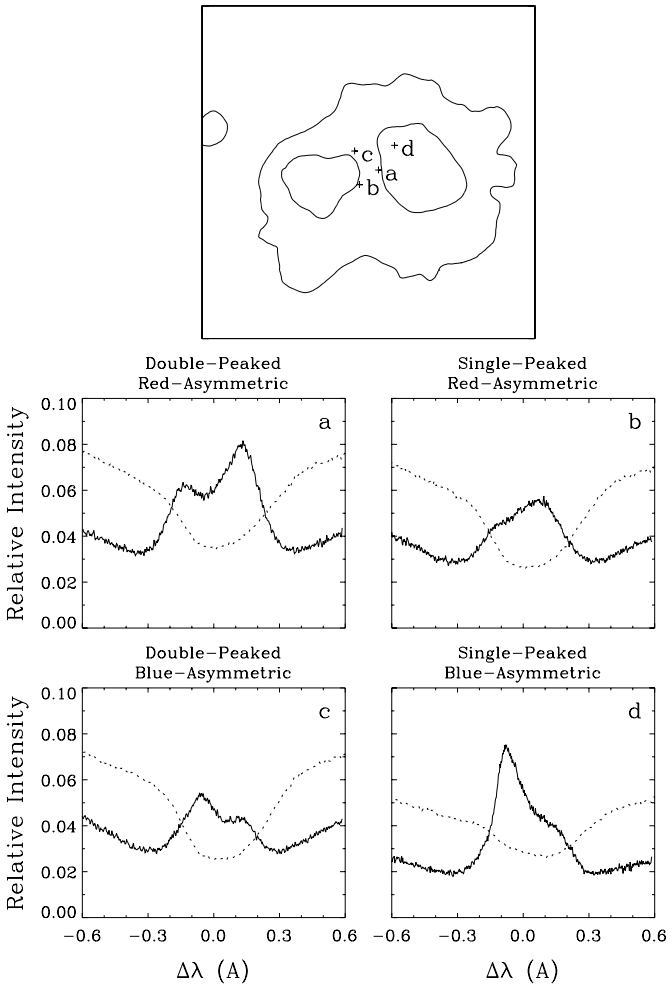

Fig. 3. Four Ca II K profiles representing typical cases of DP red-asymmetric, SP red-asymmetric, DP blue-asymmetric, and SP blue-asymmetric profiles, selected from one scan (10:01 UT). The locations for profiles are shown in the top panel, whose field of view is $33\farcs6 \times 33\farcs6$. Dotted curves correspond to Ca II 8498 lines at the same locations. Their relative intensities have been reduced by a factor of 7

hours, no great change for the shape of this asymmetry strip is found, although there seem to exist some quantitative differences.

The second thing to note is the intermittent appearance of blue asymmetry patches in the umbrae. This corresponds to an excess number of SP blue asymmetric profiles indicated in Fig. 2. Such a phenomenon can be explained by umbral flashes. However, we do not find any periodicity for a specific event. Kneer et al. (1981a) found that the flash period is about 150 s, which is too short to be detected in our 2D scanning observations.

To go into more detail, we pick up the 10:01 UT case and display in Fig. 5 the spatial distributions of A_0, A_1, A_2, and A_3 in the same way as in Fig. 4. Now it is clear that the contributions to the integrated blue asymmetry on the limb side of the penumbra come mainly from an enhanced blue minimum (K_{1v}). The blue asymmetry of K_2 does not play a great role in this asymmetry strip. However, there is evidence that the K_2 blue asymmetry is more evident on the center side of the penumbra than on the limb side. Such different spatial distributions for K_1 and K_2 asymmetries are interesting.

We do not distinguish the SP and DP profiles in displaying A_3 in Fig. 5. (One must bear in mind the completely different meanings of line center shifts in these two cases.) The results seem to reaffirm the fact revealed by Fig. 2 that the line centers (K_3) show mainly a blue shift for SP lines (see the left lowest panel). A red shift of K_3 appears preferentially in those DP lines with a strong K_2 blue asymmetry (the right lowest panel). Within the limb side asymmetry strip mentioned above, K_1 blue asymmetry prevails but no significant shift of K_3 is found.

We also derive the line bisector of the Ca II 8498 line. Like in the quiet Sun case, this line shows a slight kink towards the red wing. That is to say, the line bisector at near wing shows a red shift relative to the bisector at line center or at far wing. Nearly all the sunspot Ca II 8498 line profiles show such a behavior. The typical red shift at 70% absorption of the profile is found to be 1.6 km s^{-1}, which is larger than in the quiet Sun case. Apparently this does not reflect the real velocity in the atmosphere. No clear correlation between the asymmetries of this line and the Ca II K can be confirmed.

3.3. The influence of stray light

The observed emission from sunspots is considerably contaminated by stray light scattered from their much brighter neighborhood. The degree of contamination is of course dependent on the instrument and the atmospheric condition during observation times. To estimate the influence of stray light in the present case, we create an artificial field of stray light by convolving at each wavelength bin the spatial distribution of monochromatic intensity with a 2D Gauss function. Thus, we compute

$$I^s_\lambda = (1-p)I_\lambda + pI_\lambda * G\,, \tag{5}$$

where p measures the degree of stray light contamination. The Gauss function G has a width of $d = 15''$, a typical value found for VTT. p is set to be 0.1, which is considered as an upper limit in actual observations, as judged from limb spectra obtained on an other day with similar observing conditions.

Deriving again the asymmetry parameters described by Eqs. (1)–(4) from the artificially stray-light-contaminated spectra I^s_λ, we find only marginal changes compared with the data derived from the actually observed spectra I_λ. We thus conclude that the stray light has little influence on the general property of line asymmetries, and that the results shown in Figs. 4 and 5 can not be artifacts due to the non-correction of stray light.

3.4. Discussions

The overall feature of Ca II K line asymmetries in sunspots resembles that in the quiet Sun case in the sense that the majority of line profiles show a blue asymmetry, no matter whether the profile has double peaks or a single peak. Many authors

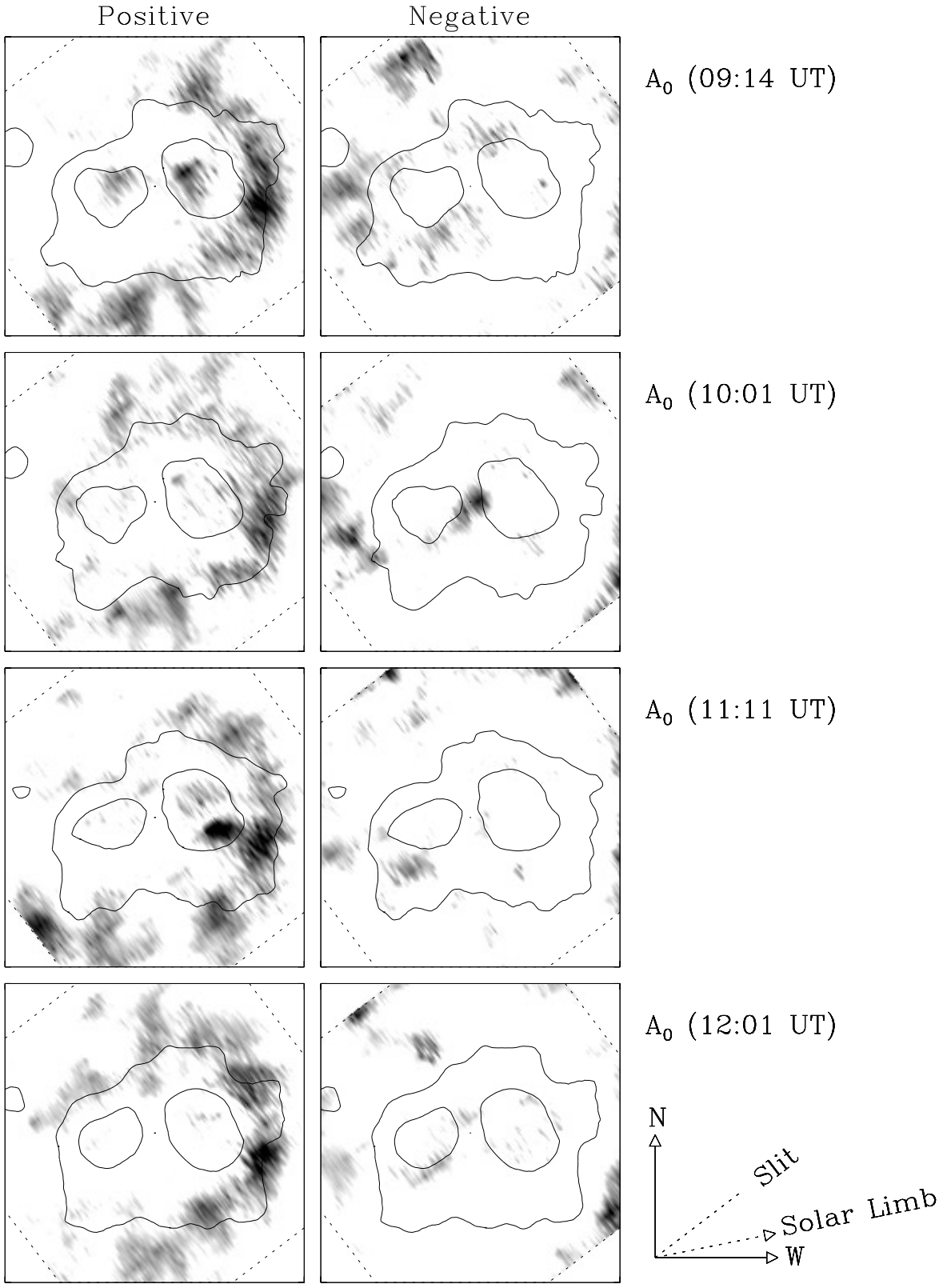

Fig. 4. Spatial distributions of A_0 in gray scale for the same four scans as in Fig. 2. The left column displays the blue asymmetry (positive A_0) while the right column shows the red asymmetry (negative A_0). Darkness 1 corresponds to $A_0 = \pm 0.30$ and darkness 0 to $A_0 = \pm 0.05$. Contours delineate the inner and outer penumbral boundaries. Dashed lines represent the slit and scanning directions. The field of view for each panel is $33\farcs6 \times 33\farcs6$

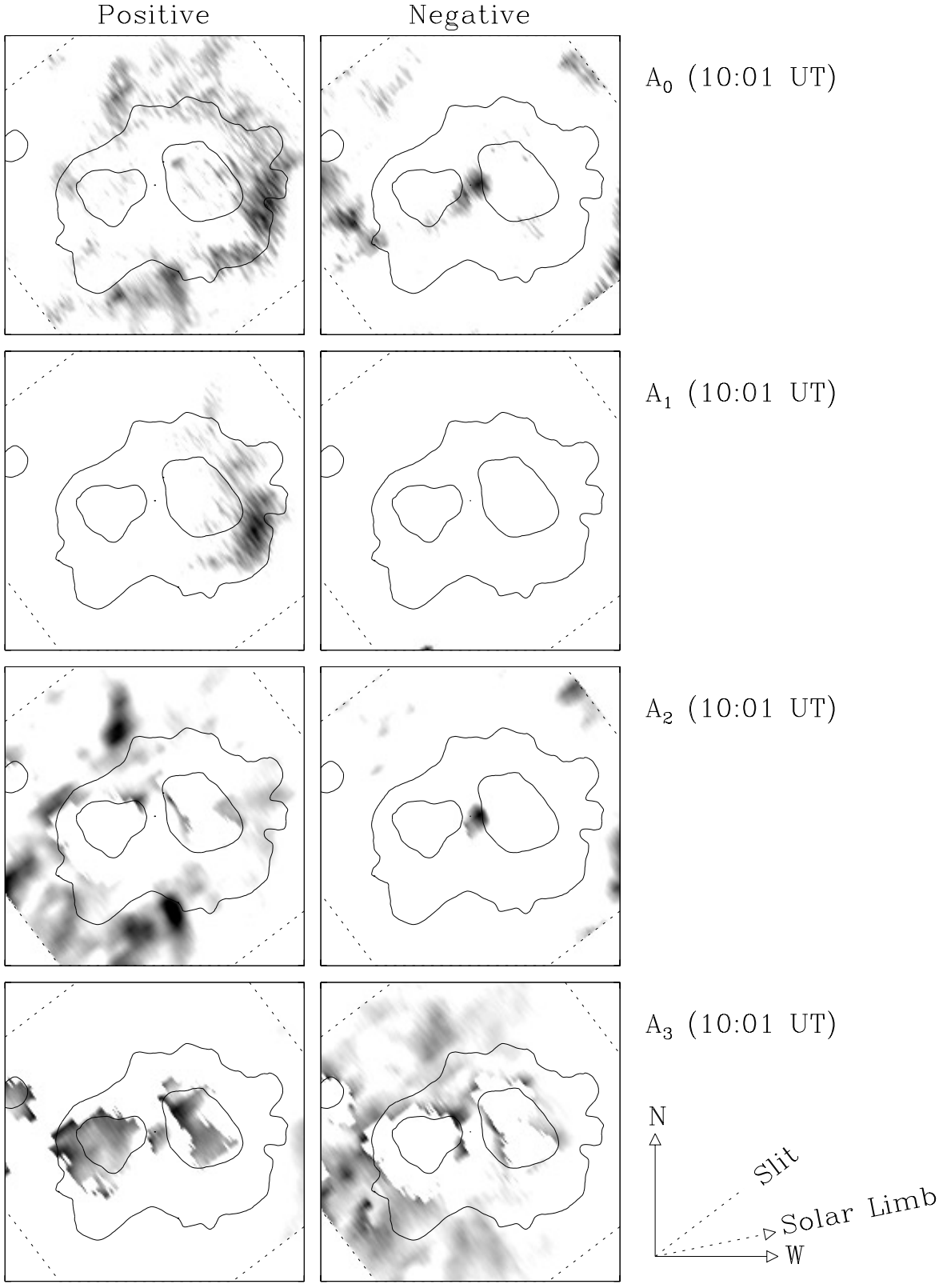

Fig. 5. Spatial distributions of A_0, A_1, A_2, and A_3 in gray scale for the 10:01 UT scan. The left column displays the positive A's while the right column shows the negative A's. Darkness 1 corresponds to $A_0 = \pm 0.30$, $A_1 = \pm 0.30$, $A_2 = \pm 0.30$, and $A_3 = \pm 0.096$ Å, and darkness 0 to $A_0 = \pm 0.05$, $A_1 = \pm 0.05$, $A_2 = \pm 0.05$, and $A_3 = \pm 0.012$ Å for the four parameters, respectively. Contours delineate the inner and outer penumbral boundaries. Dashed lines represent the slit and scanning directions. The field of view for each panel is $33\farcs6 \times 33\farcs6$

have tried to explore the origin of the Ca II K asymmetry in the quiet Sun, such as the upward propagation of acoustic waves (Heasley 1975; Cram 1976), downflow at the supergranulation cell boundaries (Linsky et al. 1979), or even dark condensations (Sivaraman 1982). However, in whatever cases, the basic point accepted by most authors is that the blue asymmetry can be produced by either an upward velocity in the K_2 forming layer or a downward velocity in the K_3 forming layer (see Durrant et al. 1976). The difference between them is that the latter also results in some red shift of K_3 while the former does not. The situation for red asymmetry is just the contrary. Of course, this basic point is still valid in explaining the asymmetry of sunspot lines.

Chromospheric oscillations have been found to exist in all solar features. According to Lites (1986, 1988), the periods of oscillations peak around 3 min in umbrae, while periods up to 24 min may be found in outer penumbrae. Profiles of Ca II resonance lines calculated from atmospheric models with non-linear oscillations (see e.g., Gouttebroze & Leibacher 1980) can exhibit considerable asymmetry. Hence, one might suspect that some of the spatial features displayed in Figs. 4 and 5 are artifacts produced by a coincidence of the stepping period with that of oscillations. In order to distinguish between the oscillatory and non-oscillatory (long-lasting) spatial features, we have also computed the average distribution of asymmetry parameters over a subset or even the whole of 12 scans, covering a time period much longer than the oscillation periods. The results are as expected: some small-scale and ephemeral features are smoothed out while the blue asymmetry patches in the penumbra, characterized by an enhanced K_{1v} on the limb side but an enhanced K_{2v} on the center side, persist. Therefore, our main interest is concentrated on the physical causes of such a steady phenomenon of line asymmetries.

The Evershed flow in sunspot penumbrae has long been known. It is considered to be nearly horizontal, outward, and confined to photospheric layers. Balthasar et al. (1996) employed a Fabry-Perot interferometer to derive a 2D velocity field around a sunspot, and found that the Evershed flow undergoes a sharp decrease at the outer penumbral boundary. In resolving the dispute of whether or not the Evershed flow extends outside the sunspot, Solanki et al. (1994) proposed a uniformed model which comprises a superpenumbral magnetic canopy carrying an outward mass flow. Such a flow can be detected outside the sunspot by lines formed in upper photospheric layers. On the limb side, the outward flow is seen away from the observer. It is certain that such a low lying flow has no influence on the Ca II K line core (K_2 and K_3). The question is thus whether it can affect the K_1 blue asymmetry which appears apparently on the limb side of the penumbra. No available line profile computations can confirm or reject this. On the other hand, it is believed that there exists inverse (inward) Evershed flow in the chromosphere (see e.g., Maltby 1975). On the center side this inward flow moves also away from the observer, thus it is favorable in explaining the observed K_2 blue asymmetry accompanied by a K_3 red shift, provided that the flow is confined to the K_3 forming layer. Moreover, it may also predict a (weak) red shift for the Ca II 8498 line, which seems to be compatible with observations.

It is possible that the K_1 blue asymmetry and K_2 blue asymmetry seen on either side of the sunspots are caused by different mass flows. However, if such flows are ascribed to some steady mechanisms, such as the Evershed or inverse Evershed flow, we should see the opposite Doppler effect (i.e., red asymmetry) on the other side. This is not the case in our observations. The geometric difference of the two sides would have some effect, but it seems unlikely that it can completely smear out such a contrast, let alone this spot is not close to the solar limb. Therefore, this problem is still open. In summary, we think that any satisfactory explanation must account for in a consistent way the line asymmetries in different line parts (K_1 and K_2), their peculiar spatial distribution and temporal evolution.

4. Conclusions

This paper presents the 2D spectral observations of sunspots in chromospheric lines. Particular attention has been paid to the line asymmetry of the Ca II K line, as well as its spatial distribution. This may provide a way to investigate the dynamics in the chromosphere above the sunspot.

Based on a statistics of line asymmetries, it is found that the majority of Ca II K profiles show a blue asymmetry, i.e., an enhanced K_{1v} or K_{2v} relative to its red wing counterpart for DP profiles, or a blue shift of K_3 for SP profiles. Red asymmetry can also appear, but only in some tiny regions and mostly short lived. There are some ephemeral blue asymmetry patches in the umbrae, which are likely to be related to umbral flashes.

On the limb side of the penumbra, the Ca II K profiles show a distinguishably blue asymmetry of K_1. In contrast, the profiles on the center side do not have such a behavior but a tendency to possess a blue asymmetry of K_2, together with a slight red shift of K_3. Like in the quiet Sun case, the latter kind of asymmetry can be explained by a downflow at the K_3 forming layer. However, there are no available computations which show how a K_1 blue asymmetry is produced, although it is reasonable that such an asymmetry indicates a velocity field confined to the temperature minimum or the upper photosphere. A further study is needed to find out a consistent explanation for the global behavior of line asymmetries in sunspots through detailed theoretical computations of line profiles.

Acknowledgements. The authors are grateful to the observing assistants, U. Abel and F. Wehmer, for their help in setting up the observing instruments. Sincere thanks are due to the referee, Dr. J.-C. Vial, for his valuable comments which help to improve the paper. M.D.D. would like to thank the staff of the Kiepenheuer-Institut for their kind hospitality during his visit there.

References

Balthasar H., Schleicher H., Bendlin C., Volkmer R., 1996, A&A 315, 603

Cram L.E., 1976, A&A 50, 263

Durrant C.J., Grossmann-Doerth U., Kneer F.J., 1976, A&A 51, 95

Gouttebroze P., Leibacher J.W., 1980, ApJ 238, 1134
Grossmann-Doerth U., Kneer F., v. Uexküll M., 1974, Solar Phys. 37, 85
Harvey K., Harvey J., 1973, Solar Phys. 28, 61
Heasley J.N., 1975, Solar Phys. 44, 275
Kneer F., Mattig W., v. Uexküll M., 1981a, A&A 102, 147
Kneer F., Scharmer G., Mattig W., Wyller A., Artzner G., Lemaire P., Vial J.C., 1981b, Solar Phys. 69, 289
Linsky J.L., Worden S.P., McClintock W., Robertson R.M., 1979, ApJS 41, 47
Lites B.W., 1986, ApJ 301, 1005
Lites B.W., 1988, ApJ 334, 1054
Liu S.-Y., Smith E.v.P., 1972, Solar Phys. 24, 301
Maltby P., 1975, Solar Phys. 43, 91
Mattig W., Kneer F., 1978, A&A 65, 11
Nye A.H., Thomas J.H., Cram L.E., 1984, ApJ 285, 381
Pasachoff J.M., 1970, Solar Phys. 12, 202
Sivaraman K.R., 1982, ApJ 254, 814
Solanki S.K., Montavon C.A.P., Livingston W., 1994, A&A 283, 221
Soltau D., 1983, The German 60 cm Vacuum Tower Telescope and its Postfocus Facilities, JOSO Annual Report
Vial J.-C., Bellout A., 1987, Publ. Astron. Inst. Czech. Acad. Sci. 66, 215

This article was processed by the author using Springer-Verlag LaTeX A&A style file *L-AA* version 3.